

# Bayesian alignment using hierarchical models, with applications in protein bioinformatics

Peter J. Green<sup>†</sup>  
University of Bristol.  
Kanti Mardia<sup>‡</sup>  
University of Leeds.

12 August 2004

## Abstract

An important problem in shape analysis is to match configurations of points in space after removing some geometrical transformation. In this paper we introduce hierarchical models for such tasks, in which the points in the configurations are either unlabelled, or have at most a partial labelling constraining the matching, and in which some points may only appear in one of the configurations. We derive procedures for simultaneous inference about the matching and the transformation, using a Bayesian approach. Our model is based on a Poisson process for hidden true point locations; this leads to considerable mathematical simplification and efficiency of implementation. We find a novel use for classic distributions from directional statistics in a conditionally conjugate specification for the case where the geometrical transformation includes an unknown rotation. Throughout, we focus on the case of a near-rigid motion transformations. Under a broad parametric family of loss functions, an optimal Bayesian point estimate of the matching matrix can be constructed, that depends only on a single parameter of the family.

Our methods are illustrated by two applications from bioinformatics. The first problem is of matching protein gels in 2 dimensions, and the second consists of aligning active sites of proteins in 3 dimensions. In the latter case, we also use information related to the grouping of the amino acids. We discuss some open problems and suggest directions for future work.

**Some key words:** bioinformatics, Markov chain Monte Carlo, matching, Poisson process, protein gels, protein structure, shape analysis, von Mises-Fisher distribution.

## 1 Introduction

Various new challenging problems in shape matching have been appearing from different scientific areas including Bioinformatics and Image Analysis. In a class of problems in Shape Analysis, one assumes that the points in two or more configurations are labelled and these configurations are to be matched after removing some transformation. Usually the transformation is a rigid transformation or similarity transformation. Several new problems are appearing where the points of configuration are either not labelled or the labelling is ambiguous, and in which some points do not appear in each of the configurations. An example of ambiguous labelling arises in understanding the secondary structure of proteins, where we are given not only the 3-dimensional molecular configuration but also the type of molecules (amino acids) at each point. A generic problem is to match such two configurations, where the matching has to be invariant under some transformation

---

<sup>†</sup>School of Mathematics, University of Bristol, Bristol BS8 1TW, UK.

Email: P.J.Green@bristol.ac.uk.

<sup>‡</sup>School of Mathematics, University of Leeds, Leeds, LS2 9JT, UK.

Email: k.v.mardia@leeds.ac.uk

group. Descriptions of such problems can be found in the review article with various references in Mardia, Taylor and Esthead (2003).

We now describe two datasets related to protein structure. One is of 2-dimensional gel data where each point is a protein itself and the transformation group is a line. In this case we have a partial matching identified already by experts, that we can use to assess our procedures. In the second example we have a 3-dimensional configuration of two active sites of two proteins which has also additional chemical information. Here the underlying transformation to be iterated out is rigid motion. In this protein structure problem, one of the main aims is to take a query active site and find matches to a given database, in some ranking order. The matches will give some idea of functions of the unknown proteins, leading to the design of new enzymes for example.

There are other related examples from Image Analysis such as matching buildings when one has multiple 2-dimensional views of 3-dimensional objects (see, for example, Cross and Hancock, 1998). The problem here requires iterating out the projective transformations before matching. Other examples involve matching outlines or surfaces (see, for example, Chui and Rangarajan, 2000, and Pedersen, 2002). Here there is no labelling of points involved, and we are dealing with a continuous contour or surface rather than a finite number of points. Such problems are not addressed in this paper.

In Section 2 we build a hierarchical Bayesian model for the point configurations and derive inferential procedure for its parameters. In particular, modelling hidden point locations as a Poisson process leads to a considerable simplification. We discuss in particular the problem when only a linear or a line transformation has to be iterated out. In Section 3 we discuss prior specifications, and provide an implementation of the resulting methodology by means of Markov chain Monte Carlo (MCMC) samplers. Under a broad parametric family of loss functions, an optimal Bayesian point estimate of the matching matrix can be constructed, which turns out to depend on a single parameter of the family. We also discuss a modification to the likelihood in our model to make use of partial label ('colour') information at the points. Section 4 describes application of our methods to the two examples from Biostatistics mentioned above: matching Protein gels in 2 dimensions and aligning active sites of Proteins in 3 dimensions. The paper concludes with some open problems and future directions.

The principal innovations in our approach are (a) the fully model-based approach to alignment, (b) the model formulation allowing integrating out of the hidden point locations, (c) the prior specification for the rotation matrix, and (d) the MCMC algorithm.

## 2 Hierarchical modelling of alignment and matching problems

We will build a hierarchical model for the observed point configurations, and derive inferential procedures for its parameters, including the unknown matching between the configurations, according to the Bayesian paradigm.

### 2.1 Point process model, with geometrical transformation and random thinning

Suppose we are given two point configurations in  $d$ -dimensional space  $\mathbb{R}^d$ :  $\mathbf{f}_{x_j}; j = 1, 2, \dots, m$  and  $\mathbf{f}_{y_k}; k = 1, 2, \dots, n$ . The points are labelled for identification, but arbitrarily.

Both point sets are regarded as noisy observations on subsets of a set of true locations  $\mathbf{f}_i$ , where we do not know the mappings from  $j$  and  $k$  to  $i$ . There may be a geometrical transformation between the  $x$ -space and the  $y$ -space, which may also be unknown. The objective is to make model-based inference about these mappings, and in particular make probability statements about matching { which pairs  $(j, k)$  correspond to the same true location? }

The geometrical transformation between the  $x$ -space and the  $y$ -space will be denoted  $A$ ; thus  $y$  in  $y$ -space corresponds to  $x = Ay$  in  $x$ -space. The notation does not imply that the transformation  $A$  is necessarily linear. It may be a rotation or more general linear transformation, a translation, both of these, or some non-rigid motion. We regard the true locations  $f_{ig}$  as being in  $x$ -space.

The mappings between the indexing of the  $f_{ig}$  and that of the data  $fx_{jg}$  and  $fy_{kg}$  are captured by indexing arrays  $f_{jg}$  and  $f_{kg}$ ; specifically we assume that

$$x_j = f_{jg} + "1_j \quad (1)$$

for  $j = 1, 2, \dots, m$ , where  $f"1_j$  have probability density  $f_1$ , and

$$y_k = f_{kg} + "2_k \quad (2)$$

for  $k = 1, 2, \dots, n$ , where  $f"2_k$  have density  $f_2$ . All  $f"1_j$  and  $f"2_k$  are independent of each other, and independent of the  $f_{ig}$ .

## 2.2 Formulation of Poisson process prior

Suppose that the set of true locations  $f_{ig}$  form a homogeneous Poisson process with rate  $\lambda$  over a region  $V \subset \mathbb{R}^d$  of volume  $v$ , and that there are  $N$  points realised in this region. Some of these give rise to both  $x$  and  $y$  points, some to points of one kind and not the other, and some are not observed at all. We suppose these four possibilities occur independently for each realised point, with probabilities parameterised so that with probabilities  $(1 - p_x - p_y - p_x p_y, p_x, p_y, p_x p_y)$  we observe neither,  $x$  alone,  $y$  alone, or both  $x$  and  $y$ , respectively. The parameter  $\lambda$  is a certain measure of the tendency a priori for points to be matched: the random thinnings leading to the observed  $x$  and  $y$  configurations can be dependent, but remain independent from point to point.

Given  $N, m$  and  $n$ , there are  $L$  matched pairs of points in our sample if and only if the numbers of these four kinds of occurrence among the  $N$  points are  $(m - n + L, m - L, n - L, L)$ . Under the assumptions above these four counts will be independent Poisson distributed variables, with means  $(v(1 - p_x - p_y - p_x p_y), vp_x, vp_y, v p_x p_y)$ . The prior probability distribution of  $L$  conditional on  $m$  and  $n$  is therefore proportional to

$$\frac{e^{-vp} x (vp_x)^m L^L}{(m - L)!} \frac{e^{-vp} y (vp_y)^n L^L}{(n - L)!} \frac{e^{-vp} p_x p_y (v p_x p_y)^L}{L!}$$

so that

$$p(L) \propto \frac{(\lambda = v)^L}{(m - L)!(n - L)L!}$$

for  $L = 0, 1, \dots, m$  in  $m$ . Here and later, we use the generic  $p(\cdot)$  notation for distributions and conditional distributions in our hierarchical model.

The matching of the configurations is represented by the matching matrix  $M$ , where  $M_{jk}$  indicates whether  $x_j$  and  $y_k$  are derived from the same point, or not, that is,

$$M_{jk} = \begin{cases} 1 & \text{if } j = k \\ 0 & \text{otherwise} \end{cases}$$

Note that  $M$  is the adjacency matrix for the bipartite graph representing the matching, and that  $\sum_{j,k} M_{jk} = L$ . We assume for the moment that conditional on  $L$ ,  $M$  is a priori uniform: there are  $\frac{m!}{L!} \frac{n!}{L!}$  different  $M$  matrices consistent with a given value of  $L$ , and these are taken as equally likely. Thus

$$p(M) = p(L)p(M|L) / \frac{(\lambda = v)^L}{(m - L)!(n - L)L!} \frac{\frac{m!}{L!} \frac{n!}{L!}}{1} / (\lambda = v)^L;$$

(where here and later  $\propto$  means proportional to, as functions of the variable(s) to the left of the conditioning  $j$  in this case,  $M$ ). Thus

$$p(M) = \frac{(\propto v)^L}{\prod_{j=0}^m \prod_{k=1}^n (\propto v)}; \quad (3)$$

Note that, because of the choice of parameterisation for the probabilities that hidden points are observed, this expression does not involve  $p_x$  and  $p_y$ .

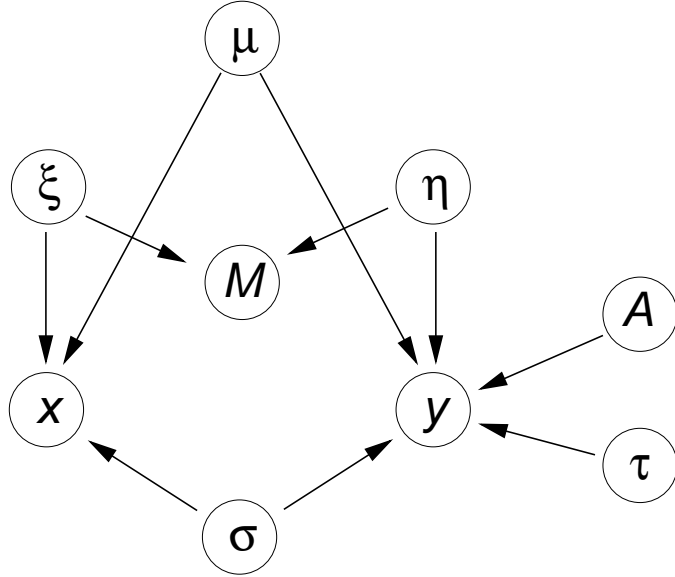


Figure 1: Directed acyclic graph representing our model, showing all data and parameters treated as variables.

### 2.3 Likelihood of data

We now have to specify the likelihood of the observed configurations of points, given  $M$ . For simplicity, we will henceforth assume that  $A$  is an affine transformation:  $A y = A y + \dots$ . From (1) and (2), the densities of  $x_j$  and  $y_k$ , conditional on  $A$ ,  $f_{1g}$ ,  $f_{2g}$  and  $f_{kg}$  are  $f_1(x_j)$  and  $\mathcal{A} f_2(A y_k + \dots)$ , respectively,  $\mathcal{A}$  denoting the absolute value of the determinant of  $A$ .

The locations  $f_{1g}$  of the  $m - L$  points that generate an  $x$  observation but not a  $y$  observation are independently uniformly distributed over the region  $V$ , so that the likelihood contribution of these  $m - L$  observations, namely  $f_{1g} : M_{jk} = 08\text{kg}$ , is

$$\int_{\substack{Y \\ j \in M_{jk} = 08k}} \int_{\substack{Z \\ V}} v^1 f_1(x_j) dV dY$$

Similarly, the contributions from the unmatched  $y$  observations, and from the matched pairs are

$$\int_{\substack{Y \\ k \in M_{jk} = 08j}} \int_{\substack{Z \\ V}} v^1 \mathcal{A} f_2(A y_k + \dots) dV dY \quad \text{and} \quad \int_{\substack{Y \\ j \in M_{jk} = 1}} \int_{\substack{Z \\ V}} v^1 f_1(x_j) \mathcal{A} f_2(A y_k + \dots) dV dY$$

respectively. These integrals all exhibit "edge effects" from the boundary of the region  $V$ , which can be neglected if  $V$  is large relative to the supports of  $f_1$  and  $f_2$ . In this case these three expressions approximate to

$$v^{(m-L)}; (\mathcal{A} f v)^{n-L}; \quad \text{and} \quad (\mathcal{A} f v)^L \int_{\substack{Y \\ j \in M_{jk} = 1}} \int_{\substack{Z \\ V}} f_1(x_j) f_2(A y_k + \dots) dV dY$$

respectively. The last expression can be written

$$(\mathbb{A} \mathbb{J} v)^L \prod_{j \in \mathbb{M}} g(x_j - A y_k) \quad (1)$$

where  $g(z) = \int_{\mathbb{R}} f_1(z+u) f_2(u) du$  (the density of  $x_j - A y_k$ ).

Combining these terms together, the complete likelihood is

$$p(x; y \mathbb{M}; A) = v^{(m+n)} \prod_{j \in \mathbb{M}} \prod_{k=1}^N g(x_j - A y_k) \quad (2)$$

Multiplying (3) and (4), we then have

$$p(\mathbb{M}; x; y \mathbb{A}) / \prod_{j \in \mathbb{M}} \prod_{k=1}^N f(x_j - A y_k) g(x_j - A y_k) \quad (3)$$

Note that the constant of proportionality involves  $m$ ,  $n$ ,  $v$ , and  $v$ , but not  $A$ ,  $\mathbb{M}$ , any parameters in  $f_1$  or  $f_2$ , or  $\mathbb{M}$  of course.

If we further specialise by making assumptions of spherical normality for  $f_1$  and  $f_2$ :

$$x_j \sim N_d(x_j; \frac{1}{x} I) \quad \text{and} \quad A y_k \sim N_d(y_k; \frac{1}{y} I);$$

with  $x = y = 1$ , say, then

$$g(z) = \frac{1}{(\frac{p}{2})^d} (z = \frac{p}{2})$$

where  $\mathbb{p}$  is the standard normal density in  $\mathbb{R}^d$ , and our final joint model is

$$p(\mathbb{M}; A; \mathbb{M}; x; y) / \prod_{j \in \mathbb{M}} \prod_{k=1}^N \frac{(f(x_j - A y_k) g(x_j - A y_k))}{(\frac{p}{2})^d} \quad (4)$$

Note that not only  $p_x$  and  $p_y$  but also  $v$  does not appear in this expression, principally from our choice of parameterisation, and that only the ratio  $p_x/p_y$  is identifiable. The directed acyclic graph representing this joint probability model, including the variables  $(\mathbb{M}, A)$  and  $(x, y)$  that we have integrated out, is displayed in Figure 1.

### 3 Prior distributions and computational implementation

We will henceforth treat  $\mathbb{M}$  and  $A$  as fixed, and consider inference for the remaining unknowns  $x$ ,  $y$  and some terms  $A$ , given the data  $f x_j g$  and  $f y_k g$ . Markov chain Monte Carlo methods must be used for the computation; several introductions and overviews of MCMC are available, for example, the primer in Green (2001).

We suppose that prior information about  $x$ ,  $y$  and  $A$  will be at best weak, and so we concentrate on generic prior formulations that facilitate the posterior analysis. Prior assumptions are therefore discussed in parallel with MCMC implementation. Note that our formulation has some affinity with mixture models, the matching matrix  $M$  playing a similar role to the allocation variables often used in computing with mixtures; see, for example, Richardson and Green (1997). As in that paper, the fully Bayesian analysis here aims at simultaneous joint inference about both the discrete and continuously varying unknowns, in contrast to frequentist approaches.

Our model has another similarity with a mixture formulation, in that as  $M$  varies, the number of hidden points needed to generate all the observed data also varies, and thus there seems to be a 'variable-dimension' aspect to the model. However, here our approach of integrating out the hidden point locations eliminates the variable-dimension parameter, so that reversible jump MCMC is not needed.

### 3.1 Priors and MCMC updating for a rotation matrix

We are interested in alignment and matching problems in which either  $A$  is given, and treated as fixed, or in which it is one of the objects of inference. In the latter case, we consider in this paper only the case of rotation matrices in two and three dimensions. We therefore focus on the full conditional distribution for  $A$ , which from (5) is

$$p(A \models ; ; ; x; y) / \models^Y_A p(A) \quad (fx_j \quad A y_k \quad g =^p 2) \\ j, k \models^Y_A j, k = 1$$

Viewing this as a density for  $A$ , we are still free to choose the dominating measure for  $p(A)$ , which is arbitrary: this full conditional density is then with respect to the same measure.

Let us restrict attention to rotations: orthogonal matrices  $A$ , (those with  $A^{-1} = A^T$ ) with positive determinant, so that  $\det A = 1$ . Expanding the expression above, we then find

$$\begin{aligned}
 & p(A) \propto \exp(-\frac{1}{2} \sum_{j=1}^n (x_j - \bar{x})^2) \\
 & p(A) \propto \exp(-\frac{1}{2} \sum_{j=1}^n (x_j - \bar{x})^2) \\
 & p(A) \propto \exp(-\frac{1}{2} \sum_{j=1}^n (x_j - \bar{x})^2) \\
 & p(A) \propto \exp(-\frac{1}{2} \sum_{j=1}^n (x_j - \bar{x})^2)
 \end{aligned}$$

Note a remarkable opportunity for (conditional) conjugacy: if  $p(A)$  has the form  $p(A) / \exp(\text{tr}(F_0^T A))$  for some matrix  $F_0$ , then the posterior has the same form with  $F_0$  replaced by

$$F = F_0 + (l=2^2) \sum_{jk} M_{jk} \delta_{jk} = 1 \quad (x_j) \quad (y_k^T)$$

This is known as the matrix Fisher distribution (Downs, 1972; Mardia and Jupp, 2000, p. 289). To the best of our knowledge, this unique role of the matrix Fisher distribution (or in the two-dimensional case, the von Mises distribution) as the prior distribution for a rotation conjugate to spherical Gaussian error distributions has not previously been noted. (Although Mardia and El-Ahmed (1976) have identified the von-Mises Fisher distribution as the conjugate prior for the mean direction). This may have relevance in models for other situations, including the simpler case where there is no uncertainty in the matching. The conjugacy is presumably related to the interpretation of the matrix Fisher distribution as a conditional multivariate Gaussian (see Mardia and Jupp, 2000, p. 289).

## Two-dimensional case

Now consider the two-dimensional case,  $d = 2$ . An arbitrary rotation matrix  $A$  can be written

$$A = \begin{pmatrix} \cos \theta & \sin \theta \\ \sin \theta & \cos \theta \end{pmatrix} !$$

and the natural dominating measure is Lebesgue measure on  $(0; 2)$  for  $\lambda$ . Then a uniformly distributed choice of  $A$  corresponds to  $p(A) / \lambda$ . More generally, the von Mises distribution for

$$p(\ ) / \exp(\cos(\ )) = \exp(\cos \cos + \sin \sin)$$

can indeed be expressed as  $p(A) / \exp(\text{tr}(F_0^T A))$ , where a (non-unique) choice for  $F_0$  is

$$F_0 = \begin{pmatrix} -2 & \cos & \sin \\ & \sin & \cos \end{pmatrix} \dots$$

Thus the full conditional distribution for  $\theta$  is of the same von Mises form, with cos updated to  $(\cos \theta + S_{11} + S_{22})$ , and sin to  $(\sin \theta + S_{12} + S_{21})$ , where  $S$  is the  $2 \times 2$  matrix  $(1 = 2^{-2}) \sum_{j,k} M_{jk}^{-1} (x_j - \theta) y_k^T$ .

It is therefore trivial to implement a Gibbs sampler to allow inference about  $A$ , assuming a von Mises prior distribution on the rotation angle (including the uniform case,  $\kappa = 0$ ). We can use the Best/Fisher algorithm, an efficient rejection method (see Mardia and Jupp, 2000, p.43), to sample from the full conditional for  $\theta$ .

### Three-dimensional case

In the three-dimensional case, we can represent  $A$  as the product of elementary rotations

$$A = A_{12} ( \begin{smallmatrix} 1 & 2 \\ 1 & 2 \end{smallmatrix} ) A_{13} ( \begin{smallmatrix} 1 & 3 \\ 1 & 3 \end{smallmatrix} ) A_{23} ( \begin{smallmatrix} 2 & 3 \\ 2 & 3 \end{smallmatrix} ) \quad (6)$$

as in Raenett and Ruedenberg (1970), and Khatri and Mardia (1977). Here, for  $i < j$ ,  $A_{ij} (i_j)$  is the matrix with  $m_{ii} = m_{jj} = \cos i_j$ ,  $m_{ij} = m_{ji} = \sin i_j$ ,  $m_{rr} = 1$  for  $r \notin i; j$  and other entries 0. We can then update each of the generalised Euler angles  $i_j$  in turn, conditioning on the other two angles and the other variables ( $M$ ;  $x$ ;  $y$ ) entering the expression for  $F$ .

The joint full conditional density of the Euler angles is

/  $\exp[\text{tr} f F^T A g] \cos 13$

for  $_{12} ; _{23} 2 ( \quad ; )$  and  $_{13} 2 ( \quad =2; =2)$ . The cosine term arises since the natural domain measure, corresponding to uniform distribution of rotation, has volume element  $\cos _{13} d _{12} d _{13} d _{23}$  in these coordinates.

Substituting the representation (6), and simplifying, we find that the trace can be written variously as  $\text{tr}FF^T A g = a_{12} \cos 1_2 + b_{12} \sin 1_2 + c_{12} = a_{13} \cos 1_3 + b_{13} \sin 1_3 + c_{13} = a_{23} \cos 2_3 + b_{23} \sin 2_3 + c_{23}$  where

$$\begin{aligned}
 a_{12} &= (\mathbf{F}_{22} \quad \sin 13F_{13}) \cos 23 + (\mathbf{F}_{23} \quad \sin 13F_{12}) \sin 23 + \cos 13F_{11} \\
 b_{12} &= (\sin 13F_{23} \quad \mathbf{F}_{12}) \cos 23 + (\mathbf{F}_{13} \quad \sin 13F_{22}) \sin 23 + \cos 13F_{21} \\
 a_{13} &= \sin 12F_{21} + \cos 12F_{11} + \sin 23F_{32} + \cos 23F_{33} \\
 b_{13} &= (\sin 23F_{12} \quad \cos 23F_{13}) \cos 12 + (\sin 23F_{22} \quad \cos 23F_{23}) \sin 12 + \mathbf{F}_{31} \\
 a_{23} &= (\mathbf{F}_{22} \quad \sin 13F_{13}) \cos 12 + (\sin 13F_{23} \quad \mathbf{F}_{12}) \sin 12 + \cos 13F_{33} \\
 b_{23} &= (\mathbf{F}_{23} \quad \sin 13F_{12}) \cos 12 + (\mathbf{F}_{13} \quad \sin 13F_{22}) \sin 12 + \cos 13F_{32}
 \end{aligned}$$

and the  $c_{ij}$  can be ignored, combined into the normalising constants. Thus the full conditionals for  $\pi_{12}$  and  $\pi_{23}$  are von Mises distributions, and so these two variables can be updated by Gibbs sampling. That of  $\pi_{13}$  is proportional to

$$\exp[a_{13} \cos \varphi_{13} + b_{13} \sin \varphi_{13}] \cos \varphi_{13}$$

and we use a random walk Metropolis update for this variable, with a perturbation uniformly distributed on  $[0.1; 0.1]$ . The latter distribution has been studied in Mardia and Gadsden (1977) but with no discussion on how to simulate a sample from it.

### 3.2 Priors and updating for other parameters

We make the standard normal/inverse gamma assumptions:

$$N_d(\cdot; \sigma^2 I)$$

and

$$\sigma^2 \sim (\cdot; \cdot);$$

Under the assumptions of (5), there is conjugacy for  $\sigma$  and  $\mathbf{M}$ , and we have explicit full conditionals:

$$\begin{aligned} \mathbf{M}^*; \mathbf{A}; \cdot; \mathbf{x}; \mathbf{y} & \sim N_d \left( \frac{\sigma^2 + \frac{P}{\sum_{j \neq k} M_{jk}} (x_j - A y_k)^2}{\sigma^2 + (d-2)L}, \frac{1}{\sigma^2 + (d-2)L} I \right) \\ \sigma^2 & \sim \frac{1}{\frac{1}{\sigma^2} + \frac{(d-2)L}{\sum_{j \neq k} M_{jk}} + \frac{(L-4)}{x_j - A y_k}} \end{aligned}$$

and so it is trivial to implement Gibbs sampler updates for these parameters.

### 3.3 Updating $\mathbf{M}$

The matching matrix  $\mathbf{M}$  is updated in detailed balance using Metropolis-Hastings moves that only propose changes to a few entries: the number of matches  $L = \sum_{j \neq k} M_{jk}$  can only increase or decrease by 1 at a time, or stay the same. The possible changes are

- (a) adding a match: changing one entry  $M_{jk}$  from 0 to 1
- (b) deleting a match: changing one entry  $M_{jk}$  from 1 to 0
- (c) switching a match: simultaneously changing one entry from 0 to 1, and another in the same row or column from 1 to 0.

The proposal proceeds as follows: first a uniform random choice is made from all the  $m+n$  data points  $\mathbf{x}_1; \mathbf{x}_2; \dots; \mathbf{x}_m; \mathbf{y}_1; \mathbf{y}_2; \dots; \mathbf{y}_n$ . Suppose without loss of generality, by the symmetry of the set-up, that an  $\mathbf{x}$  is chosen, say  $\mathbf{x}_j$ . There are two possibilities: either  $\mathbf{x}_j$  is currently matched (9k such that  $M_{jk} = 1$ ) or not (there is no such  $k$ ).

If  $\mathbf{x}_j$  is matched to  $\mathbf{y}_k$ , with probability  $p$  we propose deleting the match, and with probability  $1-p$  we propose switching it from  $\mathbf{y}_k$  to  $\mathbf{y}_{k^0}$ , where  $k^0$  is drawn uniformly at random from the currently unmatched  $\mathbf{y}$  points. On the other hand, if  $\mathbf{x}_j$  is not currently matched, we propose adding a match between  $\mathbf{x}_j$  and a  $\mathbf{y}_k$ , where again  $k$  is drawn uniformly at random from the currently unmatched  $\mathbf{y}$  points.

The acceptance probabilities for these three possibilities are easily derived from the expression (5) for the joint distribution, since in each case the proposed new matching matrix  $\mathbf{M}^0$  is only slightly perturbed from  $\mathbf{M}$ , so that the ratio  $p(\mathbf{M}^0; \cdot; \mathbf{x}; \mathbf{y})/p(\mathbf{M}; \cdot; \mathbf{x}; \mathbf{y})$  has only a few factors. Taking into account also the proposal probabilities, whose ratio is  $(1-n_u)/p$ , where  $n_u = \#\{k \mid \mathbf{x}_j \text{ is matched to } \mathbf{y}_k\}$ , we find that the acceptance probability for adding a match  $(j; k)$  is

$$\text{in } 1; \frac{(f(\mathbf{x}_j - A \mathbf{y}_k)^2)^{p/2} p^{n_u}}{((p/2)^d)} :$$

Similarly, the acceptance probability for switching the match of  $x_j$  from  $y_k$  to  $y_{k^0}$  is

$$m \in 1; \frac{(\mathbf{f}x_j \mathbf{A} y_{k^0} \mathbf{g} = \mathbf{p}^2)}{(\mathbf{f}x_j \mathbf{A} y_k \mathbf{g} = \mathbf{p}^2)}$$

and for deleting the match  $(j; k)$  it is

$$m \in 1; \frac{(\mathbf{p}^2)^d}{(\mathbf{f}x_j \mathbf{A} y_k \mathbf{g} = \mathbf{p}^2 \mathbf{p}^2 n_u^0)}$$

where  $n_u^0 = \# \text{fk } 2 \ 1; 2; \dots; n : M_{jk}^0 = 08$ . Along with just one of each of the other updates, we typically make several moves updating  $M$  per sweep, since the changes effected are so modest.

### 3.4 Loss functions

The output from the MCMC sampler derived above, once equilibrated, is a sample from the posterior distribution determined by (5). This can be reported in various ways, using numerical or graphical summaries of marginal aspects of the full joint sample.

For some purposes, however, a point estimate is desirable, and in this section we discuss obtaining a Bayesian point estimate of the matching matrix  $M$ . By standard theory, this requires specification of a loss function,  $L(M; \bar{M})$ , giving the cost incurred in declaring the matching matrix to be  $\bar{M}$  when it is in fact  $M$ . The optimal estimate given data  $(x; y)$  is the matching matrix  $\bar{M}$  that minimises the posterior expected loss

$$E[L(M; \bar{M})|x; y];$$

that is, the expectation over  $M$  being taken with respect to the posterior determined by (5).

We consider loss functions  $L(M; \bar{M})$  that penalise different kinds of error. The simplest of these are additive over pairs  $(j; k)$ . Suppose that the loss when  $M_{jk} = a$  and  $\bar{M}_{jk} = b$ , for  $a, b = 0, 1$  is ' $ab$ '; for example, ' $01$ ' is the loss associated with declaring a match between  $x_j$  and  $y_k$  when there is really none, that is, a 'false positive'. Then it is readily shown that

$$E[L(M; \bar{M})|x; y] = (\gamma_{10} + \gamma_{01} \gamma_{11} \gamma_{00}) \sum_{j,k: \bar{M}_{jk} = 1} (p_{jk} - K)$$

where

$$K = (\gamma_{01} \gamma_{00}) = (\gamma_{10} + \gamma_{01} \gamma_{11} \gamma_{00});$$

and  $p_{jk} = p(M_{jk} = 1|x; y)$  is the posterior probability that  $(j; k)$  is a match, which is estimated from an MCMC run by the empirical frequency of this match. Thus, provided that  $\gamma_{10} + \gamma_{01} \gamma_{11} \gamma_{00} > 0$  and  $\gamma_{01} \gamma_{00} > 0$ , as is natural, the optimal estimate is that maximising the sum of marginal posterior probabilities of matches  $\sum_{j,k: \bar{M}_{jk} = 1} p_{jk}$ , penalised by a multiple  $K$  times the number of matches. The optimal match therefore depends on the four loss function parameters only through the cost ratio  $K$ .

Computation of the optimal match  $\bar{M}$  would be trivial but for the constraint that there can be at most one positive entry in each row and column of the array. For modest-sized problems, the optimal match can be found by informal heuristic methods. These may not even be necessary, especially if  $K$  is not too small. In particular, it is immediate that if the set of all  $(j; k)$  pairs for which  $p_{jk} > K$  includes no duplicated  $j$  or  $k$  values, the optimal  $\bar{M}$  consists of precisely these pairs.

We could also consider loss functions that penalise mismatches directly from the sum of the losses of the individual errors. For example, declaring  $(j; k)$  to be a match when it should be  $(j; k^0)$  might deserve a relative loss greater or lesser than  $(\gamma_{10} + \gamma_{01} \gamma_{11} \gamma_{00})$ , depending on context. Such loss functions could be handled in a broadly similar way, but this is left for future work.

### 3.5 Using partial labelling information

When the points in each configuration are 'coloured', with the interpretation that like-coloured points are more likely to be matched than unlike-coloured ones, it is appropriate to use a modified likelihood that allows us to exploit such information. Let the colours for the  $x$  and  $y$  points be  $r_j^x; j = 1, 2, \dots, m$  and  $r_k^y; k = 1, 2, \dots, n$  respectively. The hidden point model is augmented to generate the point colours, as follows. Independently for each hidden point, with probability  $(1 - p_x - p_y - p_x p_y)$  we observe neither  $x$  nor  $y$  point, as before. With probabilities  $p_x$  and  $p_y$ , respectively, we observe only an  $x$  or  $y$  point, with colour  $r$  from an appropriate finite set. With probability

$$p_x p_y \sum_{r \in S} \exp f(I[r = s] + I[r \notin s]);$$

we observe an  $x$  point coloured  $r$  and a  $y$  point coloured  $s$ . Our original likelihood is equivalent to the case  $\gamma = \delta = 0$ , where colours are independent and so carry no information about matching. If  $\gamma$  and  $\delta$  increase, then matches are more probable, a posteriori, and if  $\gamma > \delta$ , matches between like-coloured points are more likely than those between unlike-coloured ones. The case  $\gamma = \delta = 1$  allows the prohibition of matches between unlike-coloured points, a feature that might be adapted to other contexts such as the matching of shapes with given landmarks.

In implementation of this modified likelihood, the MCMC acceptance ratios in Section 3.3 have to be modified accordingly. For example, if  $r_j^x = r_k^y$  and  $r_j^x \notin r_k^y$ , then the first displayed ratio has to be multiplied by  $\exp(\gamma)$  and the second one by  $\exp(\delta)$ .

Other, more complicated, colouring distributions where the log probability can be expressed linearly in entries of  $M$  can be handled similarly.

## 4 Applications

### 4.1 Matching protein gels

The objective in this example is to match two electrophoretic gels automatically, given the locations of the centres of 35 proteins on each of the two gels, displayed in Table 1. The correspondence between pairs of proteins, one protein from each gel, is unknown, so our aim is to match the two gels based on these sets of unlabelled points. We suppose it is known that the transformation between the gels is affine. In this case, experts have already identified 10 points, the first ten in each list in Table 1; see Horgan, et al (1992). Based on the information of these 10 matches, the linear part of the transformation is estimated a priori, with the consequence that if the  $y$  points, regarded as column vectors, are preprocessed by premultiplication by the matrix

$$A = \begin{matrix} & \gamma \\ & \delta \\ \begin{matrix} 0.9731 & 0.0394 \\ 0.0231 & 0.9040 \end{matrix} \end{matrix} \quad (7)$$

Dyden and Mardia (1998, pp. 2021, 292{296}), then the  $x$  and  $y$  spaces differ only in their location.

Here, we take the  $x$  and transformed  $y$  points as our starting point, and have only to make inference on the translation  $\gamma$  and the unknown matching between certain of the proteins. The model (5) will therefore be taken to apply, with  $d = 2$  and with  $A$  held fixed. The MCMC sampler described in Section 3 was run for 100 000 sweeps, after a burn-in period of 20 000 sweeps, considered on the basis of an informal visual assessment of time series traces to be adequate for convergence. Prior and hyperprior settings were:  $\gamma = 1$ ,  $\delta = 16$ ,  $\gamma = (0; 0)^T$ ,  $\delta = 20.0$  and  $\gamma = \delta = 0.0001$ . The sampler parameter  $p^2$  was set to 0.5. Such a run took about 2 seconds on a 800MHz PC. Acceptance rates for the moves updating  $M$  were between 0.6% and 2.1%.

Table 1: Gel data

index		1	2	3	4	5	6	7	8	9	10
gel 1	$x_1$	195	138	107	69	279	271	324	97	156	129
	$x_2$	367	367	311	208	104	327	320	145	259	435
gel 2	$y_1$	227	166	135	104	320	301	360	131	192	149
	$y_2$	338	336	273	159	50	295	289	89	220	412
index		11	12	13	14	15	16	17	18	19	20
gel 1	$x_1$	76	118	168	231	271	279	47	70	104	188
	$x_2$	274	321	357	229	184	224	150	75	82	183
gel 2	$y_1$	67	103	141	169	254	302	154	222	143	205
	$y_2$	284	259	291	268	329	155	174	171	18	20
index		21	22	23	24	25	26	27	28	29	30
gel 1	$x_1$	181	201	217	307	268	114	136	244	170	102
	$x_2$	82	126	88	198	152	250	249	318	221	175
gel 2	$y_1$	308	300	346	430	459	142	144	150	145	136
	$y_2$	136	31	151	52	105	386	214	154	142	49
index		31	32	33	34	35					
gel 1	$x_1$	101	114	191	245	281					
	$x_2$	109	124	33	75	88					
gel 2	$y_1$	155	150	228	198	343					
	$y_2$	67	204	31	208	40					

Table 2: The 20 marginally most probable matches in the analysis of the gel data.

rank	j	k	$p_{jk}$
1	15	21	1
2	19	19	1
3	8	8	1
4	3	3	1
5	2	2	1
6	31	30	0.9989
7	6	6	0.9987
8	4	4	0.9966
9	5	5	0.9946
10	10	10	0.9927
11	24	23	0.9855
12	7	7	0.9824
13	32	31	0.9776
14	1	1	0.9763
15	9	9	0.9677
16	26	32	0.7910
17	12	13	0.7552
18	21	33	0.3998
19	26	27	0.1931
20	35	35	0.0025

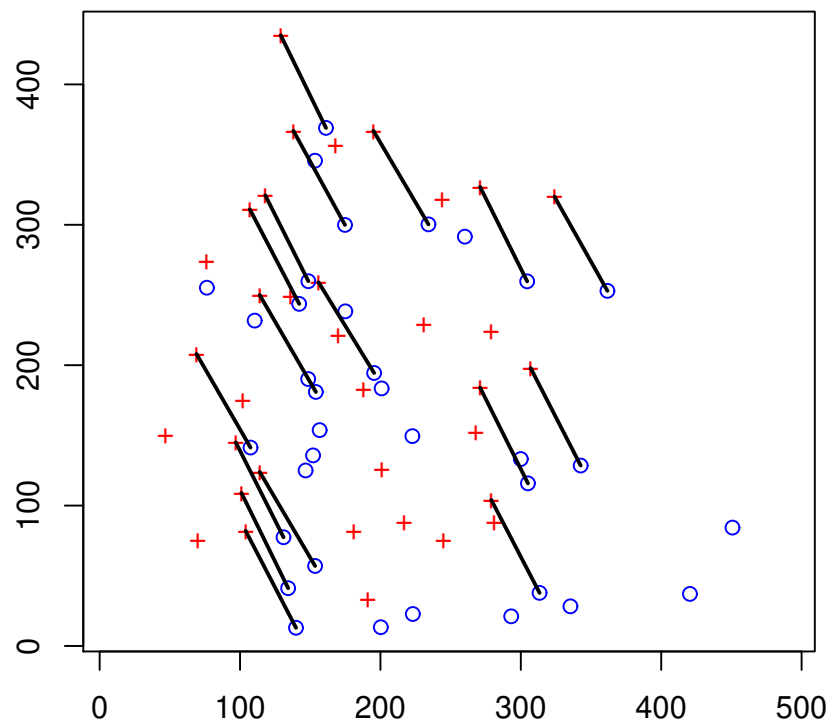


Figure 2: The 17 most probable matches in the gel data, the optimal match for any  $K = 2$   $(0.3998; 0.7552)$ ;  $+$  symbols signify  $x$  points,  $o$  symbols the  $y$  points, linearly transformed by premultiplication by the fixed affine transformation  $A$  given in (7). The solid line for each of the 17 matches joins the matched points, and represents the inferred translation plus noise.

The posterior expectation and variance of  $\theta$  were estimated to be  $(35.950, 66.685)^T$  (to be compared with  $(36.08, 66.64)^T$  obtained by Ryden and Mardia (1998)) and

$$\begin{array}{ccccc} & & & & ! \\ & 0.5776 & 0.0227 & & \\ & 0.0227 & 0.6345 & & : \end{array}$$

The posterior mean and variance of  $\theta$  are 2.050 and 0.1192.

The 20 most probable matches between  $x$  and  $y$  points are listed in Table 2; note that there is no duplication in their indices until the 19th match:  $j = 26$  also appears in the 16th match. We can conclude that for all values of  $K = (\gamma_{01} \ \gamma_{00}) = (\gamma_{10} + \gamma_{01} \ \gamma_{11} \ \gamma_{00})$  from 1 down to 0.1112, the optimal Bayesian matching is given by an appropriate subset of Table 2, reading down from the top. For example if this cost ratio is 0.8 we take the first 15 rows of the table, while if the ratio is 0.6 or 0.4 we include the 16th and 17th rows as well. The 17 most probable matches are displayed graphically in Figure 2.

It will be noted that all of the expert-identified matches, points 1 to 10 in each set, are declared to be matches with high probability in the Bayesian analysis. We also repeated the analysis with these 10 pairs held fixed. The next 9 most probable matches, together with these 10, are identical to those in the first 19 lines of Table 2, and the posterior probabilities differ by less than 0.037 in all 19 cases.

#### 4.2 Aligning proteins in three dimensions

We now apply the matching method to a problem in three dimensional structural biology, previously considered by Gold (2003). The problem consists of finding the matches for two active sites 1 and 2 corresponding to two proteins A and B respectively. Table 3 gives the corresponding coordinates  $x$  and  $y$  of these sites; these coordinates are the centres of gravity of the amino acids of the two sites. Here  $m = 40$  and  $n = 63$ . The biological details of the two proteins are as follows. Protein 1 is the human protein '17 $\beta$  hydroxysteroid dehydrogenase' and is involved in the synthesis of oestrogens. This protein binds the ligands (molecules comparatively smaller than proteins) oestradiol and NADP. Protein 2 is the mouse protein 'carbonyl reductase' and is involved in metabolism of carbonyl compounds. This protein binds the ligands 2 $\beta$ -propanol and NADP. The contact element between these two sets of ligands is NADP. From chemical properties of the sites, the relevant matching should be invariant under rigid transformation.

There is information about the identities of the amino acids in the two conformations: we defer use of this to the next section.

The MCMC sampler described in Section 3 was run for 1 000 000 sweeps, after a burn-in period of 200 000 sweeps, considered on the basis of an informal visual assessment of time series traces to be adequate for convergence. Prior and hyperprior settings were:  $\alpha = 1$ ,  $\beta = 36$ ,  $\gamma = (0; 0; 0)^T$ ,  $\delta = 50.0$ ,  $\epsilon = 0.003$  and the matrix  $F_0$  defining the prior for A set to the zero matrix. The sampler parameter  $p^2$  was set to 0.5, and we made updates to M 10 times in each sweep. Such a run took about 71 seconds on a 800MHz PC. Acceptance rates for the moves updating M were between 0.41% and 5.6%.

The posterior expectation and variance of  $\theta$  were estimated to be  $(31.60, 8.89, 17.44)^T$  and

$$\begin{array}{ccccc} 0 & & & & 1 \\ & 0.227 & 0.120 & 0.044 & \\ \theta & 0.120 & 0.307 & 0.176 \text{ \AA} & \\ & 0.044 & 0.176 & 0.428 & \end{array}$$

The posterior mean and variance of  $\theta$  are 1.051 and 0.00996. In representing the centre of the posterior distribution for the rotation matrix A, we need to use a definition of mean appropriate

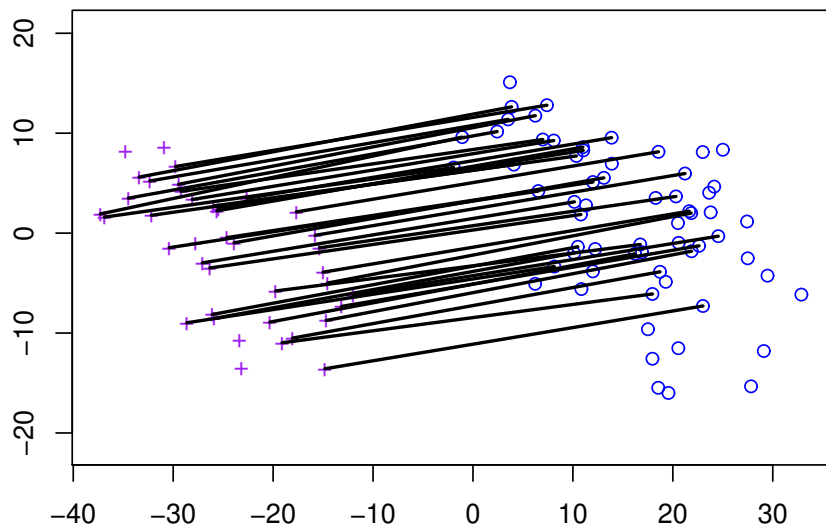


Figure 3: The optimal alignment (35 matches) when  $K = 0.7$  for the protein alignment analysis data, without using colouring information; '+' symbols signify x points, 'o' symbols the y points, rotated according to the inferred  $\hat{A}^0$  matrix given by (8). The entire joint con guration has been rotated to its rst two principalaxes. Solid lines represent the 35 marginally most probable matches, and indicate the inferred translation plus noise.

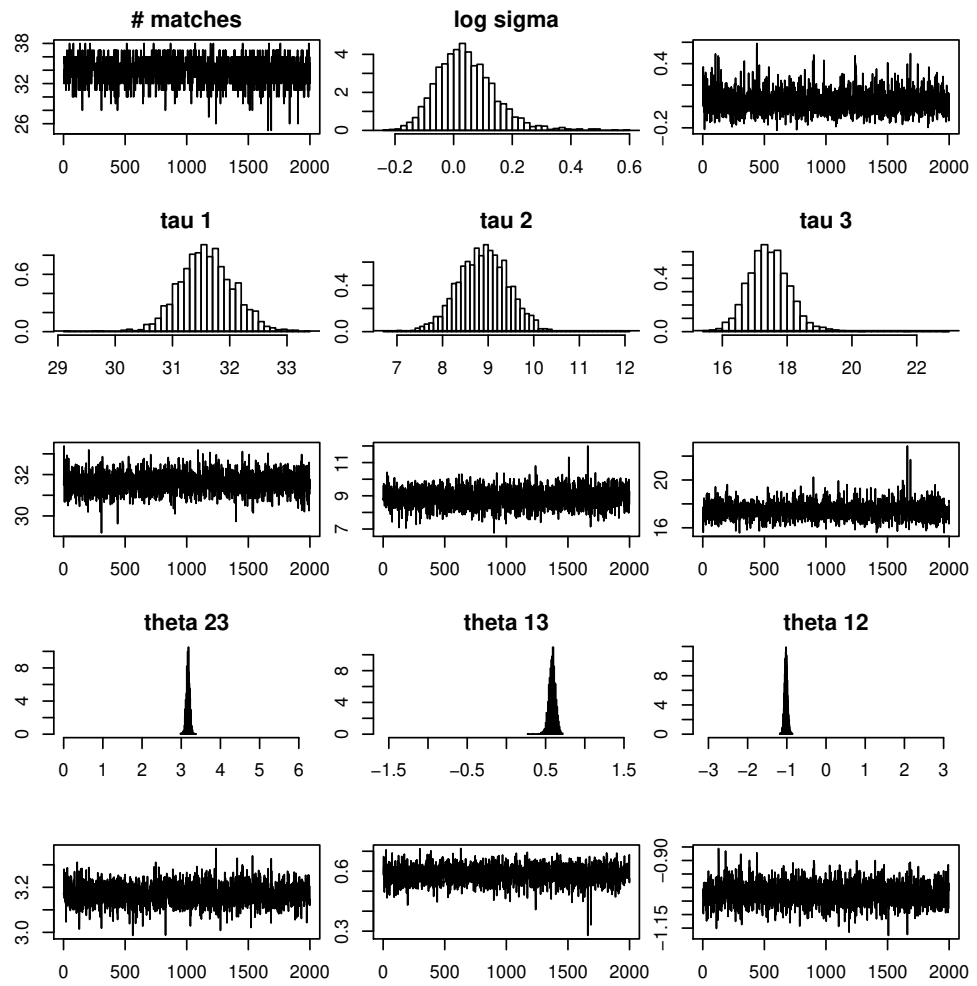


Figure 4: Time series traces and histograms of the MCMC run of Section 4.2, based on a thinned sub-sample of 2000 after burn-in.

to the geometry. We form the mean element from a thinned sample of 2000 values of  $\mathbf{A}$  from the post-burn-in MCMC run. This mean matrix  $\bar{\mathbf{A}}$  is of course not a rotation matrix, but post-multiplication by the positive definite symmetric square root of  $\bar{\mathbf{A}}^T \bar{\mathbf{A}}$  yields a rotation matrix that is known as its polar part (see Mardia and Jupp, p. 286, 290). This is an appropriate measure of location of the posterior, and takes the value

$$\bar{\mathbf{A}} = \begin{matrix} 0 & 0.4339 & 0.8444 & 0.3140 & 1 \\ \mathbf{B} & 0.7118 & 0.5350 & 0.4550 & \mathbf{C} \\ 0.5522 & 0.0261 & 0.8333 & & \end{matrix} \quad (8)$$

in this case.

The 40 most probable matches between  $\mathbf{x}$  and  $\mathbf{y}$  points are listed in Table 4; note that there is no duplication in their indices until the 39th match:  $k = 12$  also appears in the 38th match. We can conclude that for all values of  $K$  from 1 down to 0.3, the optimal Bayesian matching is given by an appropriate subset of Table 4, reading down from the top. For example if this cost ratio is 0.7 we take the first 35 rows of the table. The 35 most probable matches are displayed graphically in Figure 3; in this 3-dimensional example, the axes signify the first two principle coordinates of the combined cloud of data.

As would be anticipated, simultaneous inference for the rotation  $\mathbf{A}$  and the matching matrix  $\mathbf{M}$  (as well as  $\mathbf{x}$  and  $\mathbf{y}$ ) is a considerably greater challenge for MCMC than is the problem of the previous section, where the rotation matrix is held fixed. It is clear that there is a possibility of severe multimodality in the posterior, with the conditional posterior for  $\mathbf{M}$  and given  $\mathbf{A}$  depending strongly on  $\mathbf{A}$ . This challenge is quantified empirically by a heavy-tailed distribution of times to convergence, and by 'meta-stability' in the time series plots of various monitoring statistics against simulation time. We found the log-posterior to be a useful summary statistic for quality of fit, and pilot runs provided experience to choose a threshold value, exceedance of which we hypothesised diagnosed convergence to the main mode of the posterior.

To investigate multimodality and convergence time, we conducted a study in which the MCMC run described was repeated (with the same parameters) from 100 different initial configurations, obtained by independent random rotations as initial settings for  $\mathbf{A}$ . After short runs of 50 000 sweeps, we tested whether the threshold log-posterior value had been exceeded, and if not the run was abandoned. 83 out of the 100 runs passed this test, and these were allowed to run on for a further 450 000 sweeps. Every one of these 83 long runs provided exactly the same set of 36 most probable matches, and we therefore felt justified to conclude that they had not been trapped in a subsidiary mode of the posterior, and that it was safe to draw inference from the results. This conclusion is specific to the data set and parameter settings used, and it would be straightforward to contrive artificial data where multiple modes were more equal in probability content. In such cases more sophisticated MCMC samplers would be needed.

#### 4.3 Using information about types of amino acid

The protein alignment data includes identifiers of the type of amino acid at each point (see Table 6). There are 20 different types, which can be categorised into 4 groups: hydrophobic (1), charged (2), polar (3) and glycine (4), see Table 5; we use the group identifiers as colours in defining a modified likelihood as in Section 3.5. The parameter values taken were  $\alpha = 1.0$  and  $\beta = 0.5$ , providing a strong preference for like-coloured matching ( $\exp(-\beta) = 4.48$ ). The analysis was repeated with this modified model, leaving all other details unchanged.

The 40 most marginally probable matches are listed in Table 7, and the optimal alignment with  $K = 0.475$  displayed in Figure 5. It is interesting to note that the 35 most probable matches are

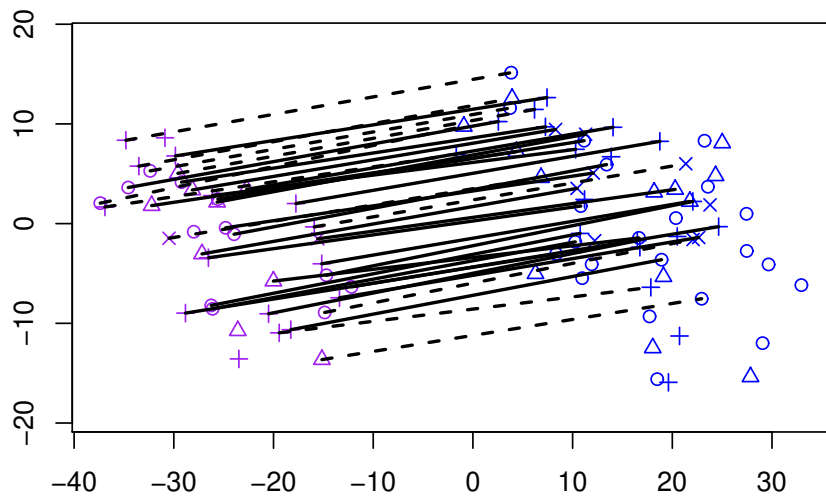


Figure 5: The optimal alignment (35 matches), when  $K = 0.475$ , in the protein alignment analysis data, using colouring information, with  $\alpha = 1.0$  and  $\beta = 0.5$ ; symbols signify the amino acid group (see Tables 6 and 5): groups 1, 2, 3 and 4 are denoted by the symbols  $\circ$ ,  $\square$ ,  $+$  and  $\triangle$ . The points have been rotated by the inferred rotation matrix  $\hat{A}$  given in (9), and the first two principal axes of the joint conformation are again used for display. The solid lines indicate the 25 matches identified by Gold (2003); our method discovers all of these, together with the 10 further matches shown with broken lines.

identical to those found in the previous section, listed in Table 4; however, there is low correlation between the orders in which these are presented, due to modest variations in the posterior probabilities attached to individual matches.

The posterior expectation and variance of  $\theta$  were now estimated to be  $(31.94; 8.94; 17.61)^T$  (slightly shifted from that obtained in the analysis of the previous section) and

$$\begin{matrix} 0 & 1.284 & 0.763 & 0.118 & 1 \\ \text{B} & 0.763 & 3.534 & 0.015 & \text{C} \\ \text{C} & 0.118 & 0.015 & 1.320 & \end{matrix}$$

The posterior mean and variance of  $\theta$  are 1.3122 and 0.1984. The increased estimate of  $\theta$  is perhaps anticipated. The centre of the posterior distribution of  $\theta$  is in this case:

$$\begin{matrix} 0 & 0.4240 & 0.8512 & 0.3092 & 1 \\ \text{B} & 0.7235 & 0.5237 & 0.4497 & \text{C} \\ \text{C} & 0.5447 & 0.0331 & 0.8379 & \end{matrix} \quad (9)$$

In the approach taken by Gold (2003) to the analysis of these data, the matching between the configurations was performed in two stages, and is not driven by an explicit probability model. First, inter-point distances  $d(\cdot, \cdot)$  were calculated within each configuration. These distances are invariant under the rigid body motions considered here. A maximum set of pairs of indices  $(j_1, k_1); (j_2, k_2); \dots$ , with no ties among the  $j$ s or  $k$ s, is found such that  $d(x_{j_r}; x_{j_s}) < d(y_{k_r}; y_{k_s})$  is less than some threshold, for all  $s \in r$ . This is done using graph theoretical algorithms of Bron and Kerbosch (1973) and Carraghan and Pardos (1990), applied to a product graph whose vertices are labelled with  $(j, k)$  pairs.

In the second stage, the matches are scored using the amino acid information, assigning a score of 1 for identity of the amino acids, and 0.5 when the amino acids are different but fall in the same group. The initial list of matches from stage one is then permuted so as to maximise the total score.

Once the matches are found the rigid body transformation is estimated by Procrustes analysis. It is interesting to compare the rotation matrix resulting from this method, namely

$$\begin{matrix} 0 & 0.441 & 0.841 & 0.312 & 1 \\ \text{B} & 0.678 & 0.541 & 0.498 & \text{C} \\ \text{C} & 0.588 & 0.008 & 0.809 & \end{matrix}$$

with that obtained by our method. The trace of the orthogonal matrix taking  $A$  to  $\hat{A}$  is approximately  $1 + 2 \cos 0.07$ , so the two differ by a rotation of only 0.07 radians. Figure 5 provides a comparison between the matchings achieved by the two approaches. Of the 25 matches identified by Gold, 18 are among the most probable 25 that we find, and all 25 are among the first 35.

## 5 Discussion

The main conclusion of this paper is that a probability model based approach is successful in allowing simultaneous inference about partial matching between two configurations of points, and a geometrical transformation between the coordinate systems in which the configurations are measured. This seems an advance over previous more ad-hoc methods.

We have only used the translation and rigid motion groups in illustrating our methodology. However, the formulation allows inference about various other group transformations such as a shear transformation, and so on. The fairly straightforward MCMC implementation presented here has

proved adequate for the models and data sets considered, although allowing rotations did increase the needed run lengths considerably. We anticipate that, at least for models allowing rotations, dealing with larger data sets will be much more challenging, since small rotational perturbations generate large displacements at sites far from the axis of rotation; moves that simultaneously perturb allocations and geometrical and error distribution parameters will be necessary for good performance. We also anticipate more severe difficulties from multimodality that were exposed in Section 4.2.

There is a need for more work in assessing the sensitivity of Bayesian inference in this setting to the prior settings used. We have only considered this issue rather informally at present. The sensitivity to  $\alpha$ ,  $\beta$  and  $\gamma$  is modest and predictable. Sensitivity to  $\delta$  is pronounced, however, as might be anticipated. This parameter ratio has a very direct role in determining whether an  $(x_j; y_k)$  pair are noisy observations of the same hidden point or not, after transformation, since it controls the density of hidden points. We should not expect to be able to draw inference about matching in practice without real prior knowledge about this ratio or an equivalent measure of the prior tendency of points to be matched.

The Poisson process for the true locations is an idealisation and there may be cases where it is not tenable, a hard core process being needed instead. For example, the minimum spacing between the centres of gravity of the amino acids in proteins is approximately eight Angstroms. Departing from the Poisson assumption would make a very substantial change to the methodology, since it would no longer be possible to integrate out the hidden point locations.

We have only used pairwise comparisons but there is scope for taking multiple combinations such as triads. The transformations considered above are parametric but some non-parametric alternatives such as non-linear deformations may be useful in some cases, eg to deal with dynamic aspects of the atoms in a protein. We have considered only two configurations but a natural extension would be to take three or more point configurations simultaneously, and make joint inference about patterns of matching between the configurations and the various geometrical transformations involved. More straightforward extensions would be to allow for non-Gaussian noise, other types of prior and so on.

In the example of Section 4.3, we used the amino acids classes in matching but there is still more information available, such as their atomic configuration. Indeed, for matching two proteins, rather than only active sites of proteins, various additional kinds of information are used in protein bioinformatics, such as the linear ordering of the amino acids and their motifs. For an excellent description see Eidhammer et al (2004) where such 3-D matching problems are termed packing patterns. The work so far is mainly algorithmic, but Wu et al (1998) provide an exception. This work uses a classical statistics framework for matching multiple protein structure. Shape distances are minimised subject to sequence information (allowing for gaps) in proteins. That is, the ranks of the atoms in a protein have been used, and the ordering is preserved allowing for the gaps. A Bayesian extension of this model has been reported in Schmidler (2004).

Kent et al (2004) have treated the unlabelled case by using a different model. While matching two configurations, one of them is taken as the population and the second as a random sample from this population after an unknown transformation. This approach is different from the symmetrical model for the two configurations proposed here. Further the emphasis in Kent et al (2004) is on maximum likelihood inference using the EM-algorithm.

Finally, in the context of using methods such as ours in database search, often the reason for assessing protein alignment, there are issues related to multiple comparisons. These are not discussed here, but the answers will depend on the size of the database as well as the number of points in the query site.

## Acknowledgements

We are grateful to Nicola Gold and Dave Westhead for their many helpful discussions, and in particular for the data in Example 2, and to Vysaul Nyirongo and Charles Taylor for various helpful comments.

## References

Bron, C. and Kerbosch, J. (1973). A lgorthm 457; nding all cliques of an undirected graph. *Commun. ACM*, 16, 575{577.

Carrahan, R. and Pardalos, P. M. (1990). Exact algorithm for the minimal clique problem. *Operations Research Letters*, 9, 375.

Chui, H. and Rangarajan, A. (2000). A new algorithm for non-rigid point matching. *IEEE Conference on Computer Vision and Pattern Recognition*, 2, 44{51.

Cross, A. D. J. and Hancock, E. R. (1998). Graph matching with dual-step EM algorithm. *IEEE transactions on pattern analysis and machine intelligence*, 20, 1236{1253.

Downs, T. D. (1972). Orientation statistics. *Biometrika*, 59, 665{676.

Dryden, I. L. and Mardia, K. V. (1998). Statistical shape analysis. Wiley, Chichester.

Edhammer, T., Jonassen, T. and Taylor, W. R. (2004). Protein Bioinformatics. Wiley, Chichester.

Gold, N. D. (2003). Computational approaches to similarity searching in a functional site database for protein function prediction. Ph.D. thesis, School of Biochemistry and Molecular Biology, University of Leeds.

Green, P. J. (2001). A Primer on Markov chain Monte Carlo, pp. 1{62 of Complex Stochastic Systems, Basmor Nielsen, O. E., Cox, D. R. and Kupperberg, C. (eds.), Chapman and Hall, London.

Horgan, G. W., Creasey, A. and Fenton, B. (1992). Superimposing two dimensional gels to study genetic variation in malaria parasites. *Electrophoresis*, 13, 871{875.

Kent, J. T., Mardia, K. V. and Taylor, C. C. (2004). Matching problems for unlabelled configurations. In *Bioinformatics, Images and Wavelets*, edited by Aykroyd, R. G., Barber, S. and Mardia, K. V. Proceedings of LASR 2004, Leeds University Press, Leeds.

Khatri, C. G. and Mardia, K. V. (1977). The von Mises-Fisher distribution in orientation statistics. *Journal of the Royal Statistical Society, B*, 39, 95{106.

Mardia, K. V. and ElAoum, S. A. M. (1977). Bayesian inference for the non-Mises-Fisher distribution. *Biometrika*, 63, 203{205.

Mardia, K. V. and Gadsden, R. J. (1977). A circle of best fit for spherical data and areas of vulcanism. *Applied Statistics*, 26, 238{245.

Mardia, K. V. and Jupp, P. E. (2000). *Directional Statistics*, Wiley, Chichester.

Mardia, K. V., Taylor, C. C., and Westhead, D. R. (2003). Structural bioinformatics revisited. In LASR 2003, pp11{18. Leeds University Press.

Pedersen, L. (2002). Analysis of two-dimensional electrophoresis gel images. PhD thesis, IMM Technical University of Denmark.

Rabenetti, R. C. and Ruedenberg, K. (1970). Parameterization of an orthogonal matrix in terms of generalized Eulerian angles. International Journal of Quantum Chemistry, IIIS, 625{634.

Richardson, S. and Green, P. J. (1997). On Bayesian analysis of mixtures with an unknown number of components (with discussion). Journal of the Royal Statistical Society, B, 59, 731{792.

Schmidler, S. C. (2004). Bayesian shape matching and structural alignment. Presentation at the 6th World Congress of the Bernoulli Society, Barcelona, July 2004.

Wu, T. D., Schmidler, S. C., Hastie, T. and Brutlag, G. (1998). Regression analysis of multiple protein structures. Journal of Computational Biology, 5, pp 585{595.

Table 3: Coordinates of the Active sites 1 and 2.

	index	1	2	3	4	5	6	7	8
site 1	$x_1$	47.297	48.89	50.774	48	44.442	42.242	44.937	51.849
	$x_2$	3.124	6.527	5.66	6.147	7.348	8.488	7.862	4.186
	$x_3$	21.673	22.166	25.364	27.923	28.422	25.57	23.009	18.012
site 2	$y_1$	11.025	9.952	8.368	4.696	6.845	7.394	6.923	14.936
	$y_2$	4.871	7.763	4.823	8.465	4.892	0.619	2.595	7.175
	$y_3$	0.16	2.125	4.003	5.391	10.564	10.226	5.55	1.208
	index	9	10	11	12	13	14	15	16
site 1	$x_1$	51.871	53.063	55.232	55.141	54.89	52.512	49.489	48.321
	$x_2$	2.283	0.915	0.358	5.983	2.04	4.657	4.19	7.742
	$x_3$	21.289	22.967	25.854	27.393	18.27	19.606	17.324	18.033
site 2	$y_1$	15.532	17.855	19.001	18.666	12.409	16.164	16.649	18.443
	$y_2$	7.818	5.625	3.613	2.704	3.386	6.563	4.763	8.564
	$y_3$	2.508	4.572	4.107	7.75	18.18	17.341	14.018	11.84
	index	17	18	19	20	21	22	23	24
site 1	$x_1$	42.241	44.352	42.349	42.692	44.371	44.403	37.155	34.387
	$x_2$	3.55	0.65	2.045	4.346	11.711	6.259	4.076	1.714
	$x_3$	19.597	20.956	22.748	25.724	22.039	19.174	19.165	20.108
site 2	$y_1$	11.985	7.456	6.434	10.655	18.051	21.652	23.632	24.082
	$y_2$	14.693	16.258	11.881	12.932	7.229	6.572	8.613	5.417
	$y_3$	4.509	7.132	14.028	16.619	6.714	7.7	5.123	3.065
	index	25	26	27	28	29	30	31	32
site 1	$x_1$	32.332	28.723	35.493	33.149	31.877	30.579	33.088	35.973
	$x_2$	1.529	1.789	7.259	3.738	6.104	4.818	4.253	6.79
	$x_3$	23.301	24.405	24.722	19.801	25.315	28.626	31.456	31.411
site 2	$y_1$	22.962	21.065	20.787	20.001	17.847	20.834	26.167	15.786
	$y_2$	1.857	0.299	2.443	11.513	13.806	16.125	14.058	13.813
	$y_3$	2.371	4.872	7.492	8.524	6.381	5.996	4.337	11.074
	index	33	34	35	36	37	38	39	40
site 1	$x_1$	41.577	43.448	40.885	37.87	36.341	29.134	28.267	33.006
	$x_2$	5.807	2.637	0.618	2.371	2.371	1.967	5.221	8.051
	$x_3$	32.609	33.586	31.636	33.166	34.675	25.013	30.82	29.247
site 2	$y_1$	13.749	10.738	8.493	14.423	14.228	12.779	12.653	8.345
	$y_2$	14.524	12.135	14.567	2.637	5.856	5.295	6.493	9.707
	$y_3$	7.956	7.944	5.933	7.11	5.148	1.662	1.961	2.62
	index	41	42	43	44	45	46	47	48
site 2	$y_1$	12.996	10.761	5.9	20.63	23.152	22.705	18.746	20.621
	$y_2$	2.001	3.973	0.544	4.149	1.038	3.783	7.927	6.145
	$y_3$	6.206	3.851	0.187	2.397	2.104	4.76	8.157	9.867
	index	49	50	51	52	53	54	55	56
site 2	$y_1$	12.235	10.206	7.165	7.752	5.831	4.948	3.64	3.836
	$y_2$	4.847	6.019	8.887	5.964	4.545	8.258	1.184	3.971
	$y_3$	5.329	8.297	2.605	2.39	1.113	1.554	9.854	7.258
	index	57	58	59	60	61	62	63	
site 2	$y_1$	5.193	2.049	4.127	2.641	2.949	12.924	12.086	
	$y_2$	0.809	1.074	2.681	2.546	3.94	6.969	8.074	
	$y_3$	5.111	4.061	1.314	0.113	4.681	7.094	3.53	

Table 4: 40 marginally most probable matches in protein alignment analysis, without using colouring information.

rank	j	k	$r_j^x$	$r_k^y$	$p_{jk}$
1	17	36	2	3	0.9325
2	7	27	2	4	0.9295
3	1	21	2	4	0.9245
4	32	44	3	3	0.9241
5	33	45	1	3	0.9237
6	23	41	3	3	0.9229
7	18	37	1	1	0.9219
8	6	26	1	1	0.9170
9	20	39	3	1	0.9128
10	31	10	3	1	0.9126
11	19	38	1	4	0.9121
12	25	1	3	2	0.9110
13	5	25	2	4	0.9107
14	24	42	3	4	0.9069
15	4	24	4	2	0.9052
16	15	34	3	3	0.9047
17	34	46	3	1	0.9046
18	30	9	1	4	0.9024
19	26	2	1	3	0.9024
20	16	35	2	3	0.8951
21	29	8	1	3	0.8943
22	2	22	1	3	0.8937
23	10	29	1	3	0.8897
24	3	23	2	2	0.8858
25	39	5	2	1	0.8730
26	35	11	1	1	0.8652
27	11	30	1	2	0.8630
28	22	40	3	3	0.8593
29	9	28	1	1	0.8531
30	40	6	3	3	0.8461
31	38	3	3	4	0.8460
32	14	33	3	2	0.7896
33	27	7	2	1	0.7847
34	12	31	3	3	0.7798
35	28	43	4	2	0.7728
36	13	32	3	1	0.6617
37	21	51	1	3	0.3240
38	36	12	2	1	0.3130
39	37	12	3	1	0.2895
40	13	33	3	2	0.0998

Table 5: Four groups of Amino acids : group 1: Hydrophobic, group 2: Charged, group 3: Polar, group 4: Glycine

Amino acid	group 1							group 2				group 3							group 4	
	A	F	I	L	M	P	V	D	E	K	R	C	H	N	Q	S	T	W	Y	G
Label	1	5	8	10	11	13	18	3	4	9	15	2	7	12	14	16	17	19	20	6

Table 6: Am into A cid types for the active sites data

index	1	2	3	4	5	6	7	8
site 1	4	1	4	6	4	5	4	14
site 2	15	17	6	11	10	12	18	2
index	9	10	11	12	13	14	15	16
site 1	13	11	13	2	14	2	7	4
site 2	6	13	5	11	18	7	15	17
index	17	18	19	20	21	22	23	24
site 1	9	1	1	7	11	14	14	12
site 2	5	10	11	4	6	2	15	15
index	25	26	27	28	29	30	31	32
site 1	12	8	15	6	10	13	14	14
site 2	6	8	6	10	14	3	16	10
index	33	34	35	36	37	38	39	40
site 1	13	2	8	4	14	14	3	7
site 2	3	17	14	12	1	6	10	17
index	41	42	43	44	45	46	47	48
site 2	16	6	9	17	16	1	9	5
index	49	50	51	52	53	54	55	56
site 2	6	10	17	12	6	10	3	17
index	57	58	59	60	61	62	63	
site 2	2	1	15	5	4	8	4	

Table 7: The 40 marginally most probable matches in the protein alignment analysis, using the colouring information, with  $\alpha = 1.0$  and  $\beta = 0.5$ .

rank	j	k	$r_j^x$	$r_k^y$	$p_{jk}$
1	6	26	1	1	0.9099
2	18	37	1	1	0.9067
3	23	41	3	3	0.9051
4	32	44	3	3	0.9016
5	3	23	2	2	0.9015
6	12	31	3	3	0.8846
7	15	34	3	3	0.8608
8	9	28	1	1	0.8471
9	40	6	3	3	0.8343
10	17	36	2	3	0.833
11	7	27	2	4	0.8132
12	1	21	2	4	0.8067
13	22	40	3	3	0.8051
14	35	11	1	1	0.7934
15	24	42	3	4	0.7712
16	2	22	1	3	0.7668
17	19	38	1	4	0.7526
18	20	39	3	1	0.7416
19	39	5	2	1	0.7323
20	10	29	1	3	0.7275
21	11	30	1	2	0.7217
22	16	35	2	3	0.7106
23	25	1	3	2	0.7103
24	29	8	1	3	0.7062
25	31	10	3	1	0.6941
26	33	45	1	3	0.672
27	30	9	1	4	0.6715
28	5	25	2	4	0.6713
29	4	24	4	2	0.6649
30	34	46	3	1	0.6608
31	26	2	1	3	0.6409
32	38	3	3	4	0.6328
33	14	33	3	2	0.5901
34	27	7	2	1	0.5165
35	28	43	4	2	0.4775
36	13	32	3	1	0.4707
37	21	51	1	3	0.2755
38	28	53	4	4	0.2748
39	36	12	2	1	0.2616
40	27	59	2	2	0.2373